



Design, Synthesis and MAO Inhibitor Activity of Chroman-4-one Derivative

Somesh Kumar Saxena ^{a*}, Ashish Pathak ^b and Om Prakash Agrawal ^a

^a Patel College of Pharmacy, Madhyanchal Professional University, Bhopal, India.

^b Ravishankar College of Pharmacy, Bhopal, India.

Authors' contributions

This work was carried out in collaboration among all authors. All authors read and approved the final manuscript.

Article Information

DOI: 10.9734/JPRI/2021/v33i63A35826

Open Peer Review History:

This journal follows the Advanced Open Peer Review policy. Identity of the Reviewers, Editor(s) and additional Reviewers, peer review comments, different versions of the manuscript, comments of the editors, etc are available here:

<https://www.sdiarticle5.com/review-history/82773>

Original Research Article

Received 25 October 2021

Accepted 27 December 2021

Published 29 December 2021

ABSTRACT

Two chalcones (4a, 4b) and nine Schiff bases (4c – 4k) of 7-hydroxy-3-formyl chromen-4-one have been synthesized. All the synthesized compounds 1–18 were screened for their hMAO (human Mono Amine Oxidase) inhibitory activity using recombinant human MAO isoforms. hMAO inhibitory activity was determined by measuring the production of H₂O₂ from p-tyramine, the common substrate for both hMAO-A and hMAO-B, using the Amplex1-RedMAO assay kit. The compounds and reference inhibitors did not react directly with the Amplex1-Red reagent indicating that they do not interfere with the measurements. The compounds were also confirmed, as they did not interact with resorufin by treating the maximum concentration of compounds with various concentrations of resorufin in order to detect if the fluorescence signal is the same with or without our compounds in the medium. No significant quenching of resorufin was observed.

Keywords: Chromanone; chalcones; schiff base; hMAO inhibitory activity.

1. INTRODUCTION

Oxygen containing heterocycles are abundantly found in nature [1]. Flavone, isoflavones, flavanones, catechins, anthocyanins are some

phytoconstituents collectively grouped as flavonoids and isoflavonoids. Chemically they are categorized as chromenes, chromenones, dihydrofurobenzofurans, chromanochromanones, benzofurochromans, xanthenes and

*Corresponding author: E-mail: somesh1207@gmail.com;

amphipyrones. Chromenones are naturally occurring compounds possessing diverse biological and pharmacological activities. Many synthetic analogues of chromenones have been evaluated for their anticancer, anticonvulsant, angioprotective, antiallergic, antihistaminic, antimicrobial, antioxidant, anti-HIV9 activities.

Due to emergence of multi-drug-resistant strains of microbes like methicillin resistant staphylococcus aureus (MRSA), vancomycin resistant enterococci (VRE), multidrug resistant mycobacterium tuberculosis (MRD-TB) and penicillinase producing *Neisseria gonorrhoeae* (PPNG), microbial diseases have become more complex to tackle. Many synthetic and semi-synthetic antimicrobial drugs have been discovered and used in clinical practice [2-5]. In spite of significant developments in antimicrobial therapy, the problem of drug resistance, spectrum of activity, potency, safety and toxicity remain unresolved. Many quinolones and fluoroquinolones like Norfloxacin, Lomefloxacin, Enoxacin, Ofloxacin, Ciprofloxacin, Levofloxacin, Sparfloxacin, Gatifloxacin, Moxifloxacin, Garenoxacin and Moxifloxacin are used in clinical practice. Structurally 4-quinolones and 4Hchromen-4-ones are very similar in many respects. Calchones¹¹ and Schiff's bases¹² of heterocyclic compounds are also versatile molecules possessing antimicrobial activity [6-8]. Based on above impetus we attempted the synthesis of chalcones and Schiff bases of 4H-chromen-4-ones (benzopyran-4-ones). 7-Hydroxy-3-formyl chromen-4-one was synthesized from 2,4-dihydroxy acetophenone by reported method¹³.

Two calchones with various aromatic ketones (4a, 4b) were synthesized by Claisen Schmidt condensation of 7-hydroxy-3-formyl chromen-4-one with substituted acetophenones by base catalyzed reaction followed by dehydration and nine Schiff bases (4c-4k) were prepared. All the synthesized chalcones and Schiff bases were evaluated for their antimicrobial activity against two Gm+ organisms (*Staphylococcus aureus*, *Bacillus subtilis*) and two Gram-negative organisms (*Escherichia coli*, *Pseudomonas aeruginosa*).

2. MATERIALS AND METHODS

2.1 Experimental

The following strategies have been used to find potent monoamine oxidase-B inhibitors.

1. QSAR studies of some reported monoamine oxidase-B inhibitors by using pharmacophore model.
2. Synthesis and biological evaluation of some *(Z)*-3-ethylidene-5,7-dimethylthiochroman-4-one and *(Z)*-2-ethylidene-4,6-dimethylbenzofuran-3(2H)-one derivatives.
 - I. *Design and Docking studies of newly designed molecules*
 - II. *Synthesis of (Z)-3-ethylidene-5,7-dimethylthiochroman-4-one and (Z)-2-ethylidene-4,6-dimethylbenzofuran-3(2H)-one derivatives.*
 - III. *In vitro evaluation of monoamine oxidase-B inhibitory activity.*
 - IV. *In vivo biological evaluation.*
3. ADME studies of newly synthesized molecules

2.2 The Work Station

The calculations were performed on hp PC running on Pentium-D processor.

2.3 Software

The present work was performed on Schrodinger (maestro 9) software using phase module, which is a versatile product for pharmacophore perception, structure alignment, activity prediction, and 3D database searching. Given a set of molecules with high affinity for a particular protein target, Phase uses fine-grained conformational sampling and a range of scoring techniques to identify common pharmacophore hypotheses, which convey characteristics of 3D chemical structures that are purported to be critical for binding. Each hypothesis is accompanied by a set of aligned conformations that suggest the relative manner in which the molecules are likely to bind.

2.3.1 Phase consists of the following four workflows:

- Building a pharmacophore model (and an optional QSAR models) from a set of ligands.
- Building a pharmacophore hypothesis from a single ligand (and editing it).
- Preparing a 3D database that includes pharmacophore information.
- Searching the database for matches to a pharmacophore hypothesis.

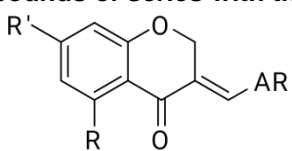
2.4 QSAR Study

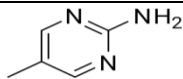
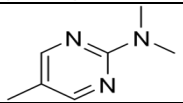
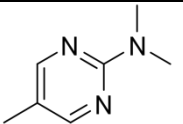
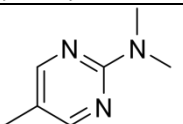
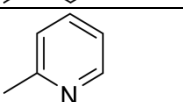
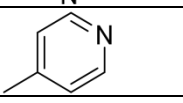
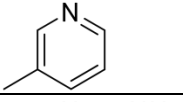
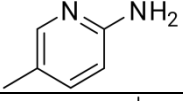
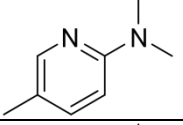
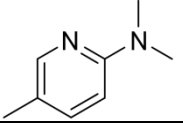
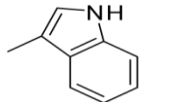
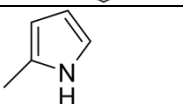
2.4.1 Selection of data set

Nicoletta Desideri *et al* developed the series (E)-3-Heteroarylidenechroman-4-ones as potent and selective monoamine oxidase-B inhibitors. The

series consist of total 18 numbers of compounds with well defined monoamine oxidase-B inhibitory activity. The IC₅₀ values were chosen for generating common pharmacophore hypotheses and 3D-QSAR study. The compounds of series with their inhibition data are detailed in table below.

Table 1. The compounds of series with their inhibition data



Comp. Name	R	R'	Ar	hMAO-B (IC ₅₀)
1A	H	H		18.33
1B	H	H		.24
1C	Cl	Cl		.01
1D	H	OCH ₃		10.40
1E	H	H		2.94
1F	H	H		12.44
1G	H	H		8.23
1H	H	H		2.39
1I	H	H		.21
1J	Cl	Cl		10.51
1K	H	H		.18
1L	H	H		13.76

Comp. Name	R	R ¹	Ar	hMAO-B (IC ₅₀)
1M	H	H		20.20
1N	Cl	Cl		10.21
1O	H	OCH ₃		10.62
1P	H	H		3.77
1R	H	H		1.13
1Q	H	H		1.73

2.4.2 Ligand preparation for pharmacophore model development

Developing a pharmacophore model requires all-atom 3D structures that are realistic representations of the experimental molecular structure. The 3D structures of compounds in the series were sketched using maestro and the sketched structures were energy minimized/cleaned up in same software in phase for the following actions:

- Convert structures from 2D to 3D.
- Add hydrogen atoms to ensure that the structure is an all-atom structure.
- Remove counter ions and water molecules.
- Add or remove protons to produce the most probable ionization state at the target pH.
- Generate Stereoisomers as different stereoisomers may exhibit different pharmacophore models.
- Remove noncompliant structures from database.
- Perform an energy minimization using the minimize option in the Impref minimization panel of Protein Preparation Wizard.

2.4.3 Generation of the conformers

Conformers for all ligands were generated in generate conformer option by fulfilling all the conditions to generate conformers.

2.4.4 Defining the ligand set for model development

In this option the sketched ligands were assigned active and inactive in activity threshold after converting the IC₅₀ values in $-\text{Log}_{10}\text{IC}_{50}$.

2.4.5 Pharmacophore sites creation

This step was performed in the Create Sites step of the 'Develop Pharmacophore Model' panel. The following sites were created for the pharmacophore:

- Hydrogen bond acceptor (A)
- Hydrogen bond donor (D)
- Hydrophobic group (H)
- Negatively charged group (N)
- Positively charged group (P)
- Aromatic ring (R)

2.4.6 Finding common pharmacophores

This step was performed in the 'Find Common Pharmacophores' option by keeping maximum and minimum number of sites-5 and specifying the number of actives to match in the 'Must match' section and selecting variants from the Variant list in the dialogue box. Pharmacophores from all conformations of the ligands in the active set were examined, and those pharmacophores that contain identical sets of features with very similar spatial arrangements were grouped together by the PHASE [9,10]. Common pharmacophore hypotheses were identified using

conformational analysis and a tree-based partitioning technique. The resulting pharmacophores were then scored and ranked. Pharmacophores with high-ranking scores were validated by a partial least square (PLS) regression-based.

2.4.7 Scoring the hypotheses

In the 'Score Hypotheses' step, common pharmacophores were examined, and a scoring procedure was applied to identify the pharmacophore from the best alignment of the chosen actives and provided a ranking of the different hypotheses for the next step.

2.5 QSAR Model Development

For build up a 3D-QSAR model a best hypothesis was selected and model was build up in following steps:

- Displayed the ligands in the Alignments table.
- Selected the training set and the test set by applying 50% as random training set.
- Set parameters in the Build QSAR Model - Options dialog box.

2.5.1 Determination of hMAO-A and -B activities

The activities of hMAO-A and hMAO-B were determined using p-tyramine as common substrate and calculated as 177.00-9.55 pmol/mg/min (n = 3) and 140.90 11.70

pmol/mg/min (n = 3), respectively. The interactions of the synthesized compounds with hMAO isoforms were determined by a fluorimetric method described and modified previously activity [11, 12]. The production of H₂O₂ catalyzed by MAO isoforms was detected using Amplex1- Red reagent, a non-fluorescent, highly sensitive, and stable probe that reacts with H₂O₂ in the presence of horseradish peroxidase to produce the fluorescent product resorufin. The reaction was started by adding (final concentrations) 200 mmol/L Amplex Red reagent, 1 U/mL horseradish peroxidase, and p-tyramine (concentration range 0.1–1 mmol/L). Control experiments were carried out by replacing the synthesized compound and reference inhibitors. The possible capacity of compounds to modify the fluorescence generated in the reaction mixture due to nonenzymatic inhibition was determined by adding these compounds to solutions containing only the Amplex Red reagent in a sodium phosphate buffer.

3. RESULT AND DISCUSSION

3.1 Results of 3D-Qsar Study (Pharmacophore Model Generation)

The pharmacophore model was generated by the PHASE with following features:

- Two hydrogen bond acceptors (A)
- One aromatic ring hydrogen bond donor (D)

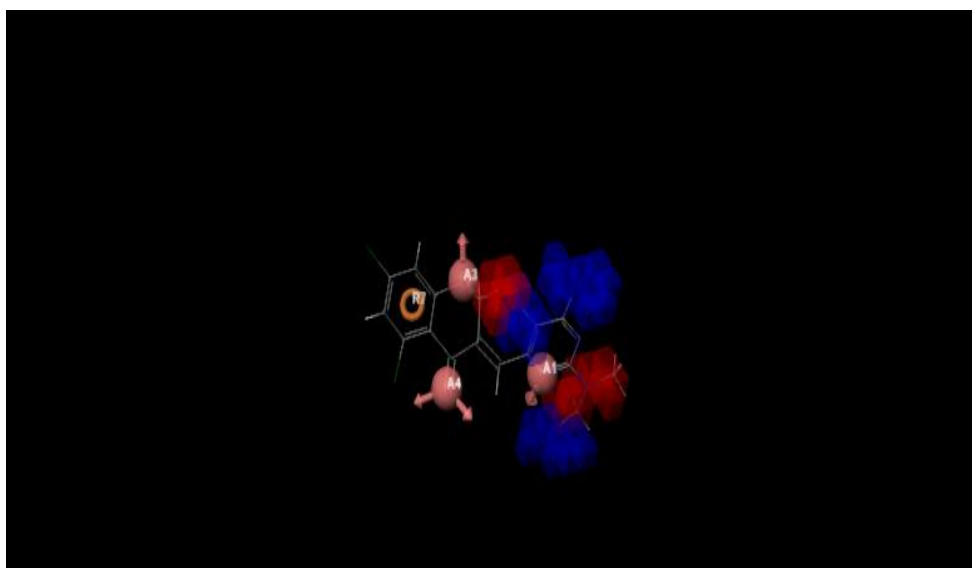


Fig. 1. A Common Pharmacophore of the active Ligands (three H- donor & two H-acceptor)

For build up a 3D-QSAR model a best hypothesis -AAR.4334 was selected and model was built by assigning PLS factor-3 on the basis of formula.

=No. of training set compounds/5(model containing 21 no. of training set compounds).

Table 2. Score of different parameters of the hypothesis- AAR-4334

S. No.	Parameters	Score
1	Survival	3.73
2	Survival inactive	1.831
3	Post-hoc	3.73
4	Site	0.96
5	Vector	1
6	Volume	0.766
7	Selectivity	1.691
8	Matches	13
9	Energy	2.879
10	Activity	4.452
11	Inactive	1.9

Where,

3.1.1 Survival

Weighted combination of the vector, site, volume, and survival scores, and a term for the number of matches.

3.1.2 Survival inactive

Survival score for actives with a multiple of the survival score for inactive subtracted.

3.1.3 Post-hoc

This score is the result of rescoring, and is a weighted combination of the vector, site, volume, and selectivity scores.

3.1.4 Site

This score measures how closely the site points are superimposed in an alignment to the pharmacophore of the structures that contribute to the hypothesis, based on the RMS deviation of the site points of a ligand from those of the reference ligand.

3.1.5 Vector alignment score

This score measures how well the vectors for acceptors, donors, and aromatic rings are

aligned in the structures that contribute to the hypothesis, when the structures themselves are aligned to the pharmacophore.

3.1.6 Volume

Measures how much the volume of the contributing structures overlap when aligned on the pharmacophore. The volume score is the average of the individual volume scores.

The individual volume score is the overlap of the volume of an aligned ligand with that of the reference ligand, divided by the total volume occupied by the two ligands.

3.1.7 Selectivity

Estimate of the rarity of the hypothesis, based on the World Drug Index. The selectivity is the negative logarithm of the fraction of molecules in the Index that match the hypothesis. A selectivity of 2 means that 1 in 100 molecules match. High selectivity means that the hypothesis is more likely to be unique to the actives.

3.1.8 Matches

Number of actives that match the hypothesis.

3.1.9 Energy

Relative energy of the reference ligand in kcal/mol. This is the energy of the reference conformation relative to the lowest-energy conformation.

3.1.10 Activity

Activity of the reference ligand.

3.1.11 Inactive

Survival score of inactive. The scoring function is the same as for actives. The large value of survival score indicates the better fitness of the active ligands on the common pharmacophore and validates the model.

Table 3. 3D-QSAR statistical parameters

S. No.	SD	R-squared	F	P	RMSE	Q-squared	Pearson-R
1	0.089	0.953	108.6	7.52E-11	0.549	0.389	0.262
2	0.075	0.978	240.1	1.64E-13	0.397	0.143	0.381
3	0.057	0.988	422.8	1.92E-15	0.402	0.618	0.524
4	0.046	0.992	757.8	1.90E-17	0.343	0.793	0.827

Where-

- SD- Standard deviation of the regression.
- R-squared Value of R^2 for the regression.
- F- Variance ratio. Large values of F indicate a more statistically significant regression
- P- Significance level of variance ratio. Smaller values indicate a greater degree of Confidence.
- RMSE- Root-mean-square error.
- Q-squared Value of Q^2 for the predicted activities.
- Pearson-R Pearson R value for the correlation between the predicted and observed activity for the test set.

The large value of F indicates a statistically significant regression model, which is supported by the small value of the variance ratio (P), an indication of a high degree of confidence.

Table 4. Fitness and predicted activity for test and training set of compounds

Ligand Name	QSAR Set	# Factors	Predicted Activity	Pharm Set	Fitness
1 a	test	1 2 3	4.91 4.93 5.01	active	1.88
1 b	training	1 2 3	5.04 5.02 5.09	active	2.67
1 c	test	1 2 3	5.01 4.97 5.02	active	2.65
1 d	training	1 2 3	4.99 4.96 5.00	active	2.7
1 e	test	1 2 3	4.96 4.94 4.98	active	2.58
1 f	test	1 2 3	4.54 4.68 4.56	inactive	0.56
1 g	training	1 2 3	4.66 4.51 4.52	active	3
1 h	training	1 2 3	4.68 4.54 4.56	active	2.83
1 i	test	1 2 3	4.79 4.65 4.66	active	2.73
1 j	test	1 2 3	4.80 4.67 4.68	active	2.74
1 k	test	1 2 3	4.87 4.73 4.75	active	2.71
1 l	training	1 2 3	4.85 4.68 4.68	active	2.7
1 m	training	1 2 3	4.63 4.49 4.50	active	2.92
1 n	test	1 2 3	4.69 4.55 4.56	active	2.85
1 o	test	1 2 3	4.75 4.60 4.61	inactive	2.76
1 p	test	1 2 3	4.79 4.63 4.64	inactive	2.79

The large value of predicted activity and fitness for the active ligands also validate the model for activity prediction of newer analogs.

The following figures show 3D-pharmacophore regions around compounds. The blue and red cubes refer to ligand regions in which a molecular substitution with a specific feature behavior, respectively, increases or decreases binding affinity for the target.

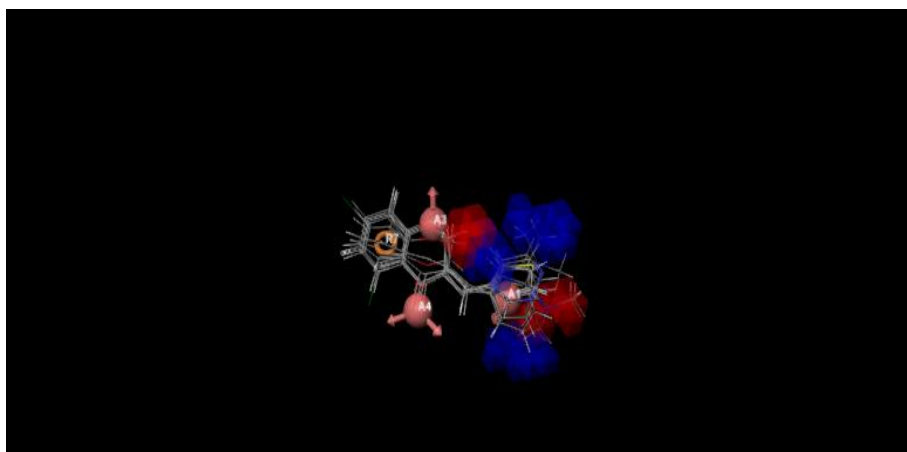


Fig. 2. Alignment of active ligands on *pharmacophore* region

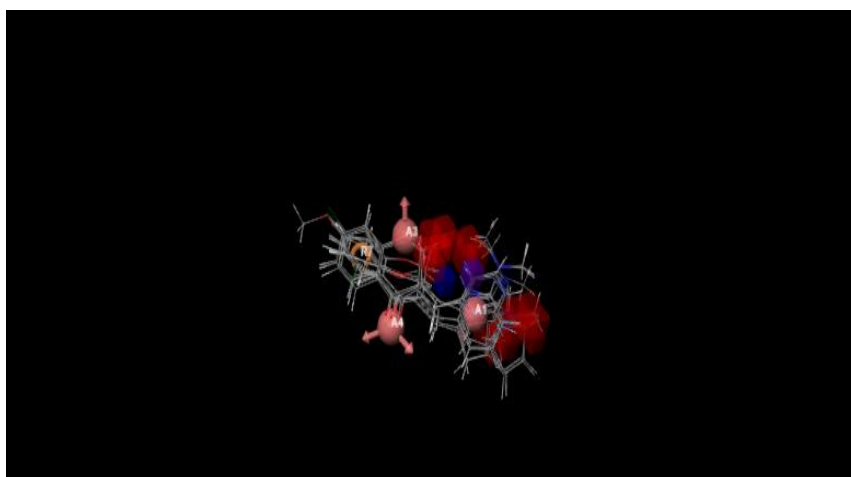


Fig. 3. Alignment of inactive ligands on pharmacophore region

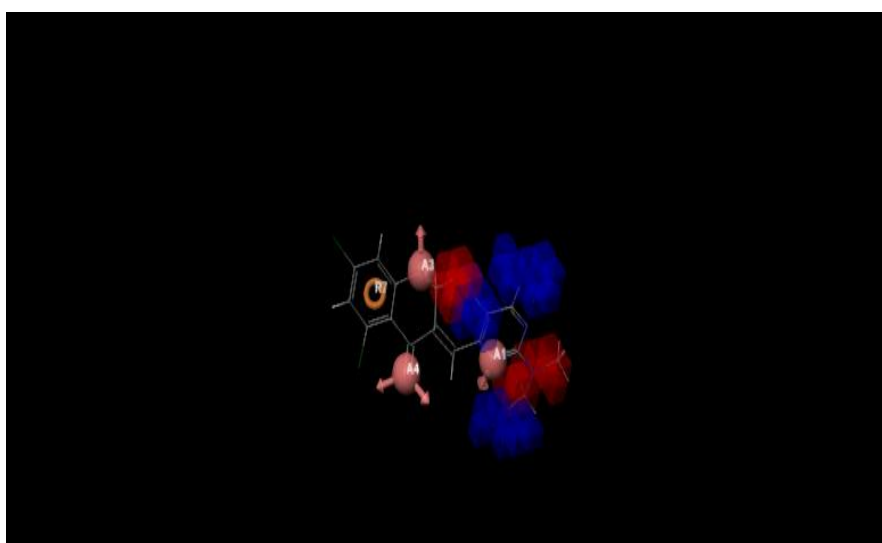


Fig. 4. Alignment of most active ligands on pharmacophore region

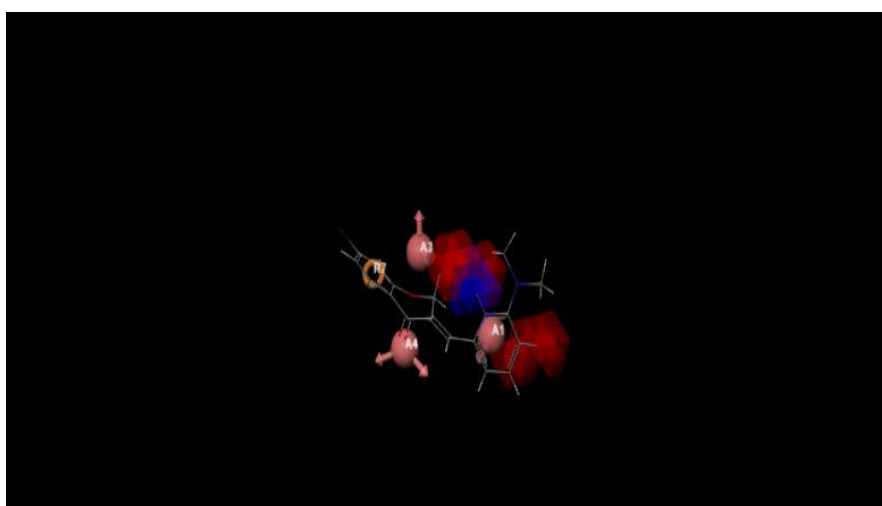


Fig. 5. Alignment of Inactive ligands on pharmacophore region

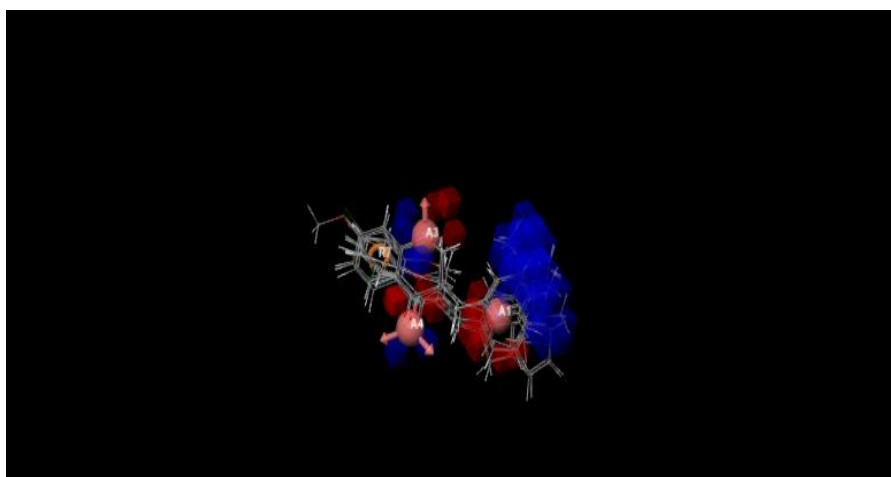


Fig. 6. Electron withdrawing feature

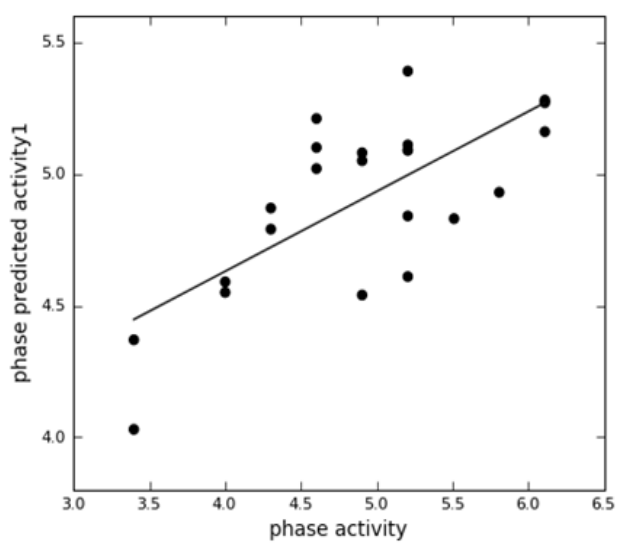


Fig. 7. Phase activity v/s Phase predicted activity for test set of ligands

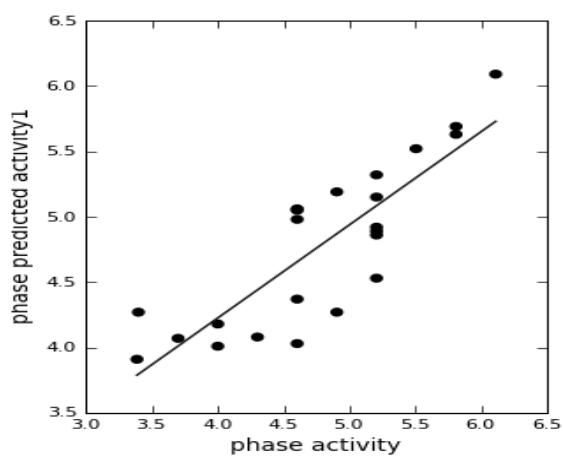


Fig. 8. Phase activity v/s Phase predicted activity for training set of ligands

All the synthesized compounds 1–18 were screened for their hMAO inhibitory activity [11, 12] using recombinant human MAO isoforms. hMAO inhibitory activity was determined by measuring the production of H₂O₂ from p-tyramine, the common substrate for both hMAO-A and hMAO-B, using the Amplex1-RedMAO assay kit. The compounds and reference inhibitors did not react directly with the Amplex1-Red reagent indicating that they do not interfere with the measurements [13-16]. The compounds were also confirmed, as they did not interact with resorufin by treating the maximum concentration of compounds with various concentrations of resorufin in order to detect if the fluorescence signal is the same with or without our compounds in the medium. No significant quenching of resorufin was observed. The experimental data concerning to the inhibition of hMAO-A and hMAO-B inhibition by the novel compounds 1–18 were presented in Table 1, together with their selectivity indices. The selectivity index was expressed as $SI = K_i(\text{MAO-A})/K_i(\text{MAO-B})$ for selectivity towards hMAO-B. Protein was determined according to the method of Bradford method [17] using bovine serum albumin as the standard.

Compounds, 1–5, 7–17 and 19 were found to inhibit hMAO-B selectively and reversibly, while, compound 18 having bulkier aldehyde portion (anthracen-9-yl) was found to be competitive, reversible and selective inhibitor of hMAO-A isoforms with $K_i=0.11_{-0.01}\text{mmol/L}$, while compound 6 and 20 which carrying 4-NO₂, and thiophen-2-yl were found to be nonselective towards the MAO isoforms. The most potent MAO-B inhibitor in this series was compound 17 ($K_i=0.10_{-0.01}\text{mmol/L}$), which was carrying naphth-2-yl group at aldehyde position. It was also found to have potency and selectivity almost equal to selegiline, a well-known selective MAO-B inhibitor ($K_i=0.12_{-0.01}\text{mmol/L}$), Compound 14 which was carrying 3,4-diOMe functional group exhibited the best selectivity ($SI = 26.14$) towards hMAO-B. The activity profiles of this series of compounds were then compared with their flavones counterparts reported earlier by our group [18]. In spite of structural variation viz: (i) fused furan in place of pyran and (ii) exocyclic double bond in place of endocyclic double bond, this series displayed similar activity profile as that of their flavone counterparts in potency as well as selectivity towards MAO isoforms.

5. CONCLUSION

A series of eighteen 2-(arylmethylidene)-2,3-dihydro-1-benzofuran-3-one derivatives were synthesized and screened for their potential to inhibit hMAO isoforms selectively. With the limited variations at single site, benzylidene portion the activity profile was recorded and a concise SAR was derived. In summary, weak to moderate electron pumping as well as electron withdrawing groups favor selectivity towards hMAO-B, while strong deactivators make them non-selective towards isoforms. Mono-substitution of methoxy group at o- and m-position increases potency while bi-substitution lead to the improved potency as well as selectivity.

DISCLAIMER

The products used for this research are commonly and predominantly use products in our area of research and country. There is absolutely no conflict of interest between the authors and producers of the products because we do not intend to use these products as an avenue for any litigation but for the advancement of knowledge. Also, the research was not funded by the producing company rather it was funded by personal efforts of the authors.

CONSENT

It is not applicable.

ETHICAL APPROVAL

It is not applicable.

COMPETING INTERESTS

Authors have declared that no competing interests exist.

REFERENCES

1. Robert Knapp D. Cheese and monoamine oxidase inhibitors Headache. J. Head Face Pain. 1964;3;157–158.
2. Blackwell B. Hypertensive crisis due to monoamine-oxidase inhibitors, Lancet. 1963;282:849–851.
3. Morales-Camilo N, Salas CO, Sanhueza C, et al. Synthesis, biological evaluation, and molecular simulation of chalcones and aurones as selective MAO-B inhibitors. Chem. Biol. Drug Des. 2015;85:685–695.

4. Chimenti F, Fioravanti R, Bolasco A, et al. A new series of flavones, thioflavones, and flavanones as selective monoamine oxidase-B inhibitors, *Bioorg. Med. Chem.* 2010;18:1273–1279.
5. Badavath VN, Ciftci-Yabanoglu S, Jadav SS, Jagrat M, Sinha BN, Ucar G, Jayaprakash V. Monoamine oxidase inhibitory activity of 3,5-biaryl-4,5-dihydro-1H-pyrazole-1-carboxylate derivatives, *Eur. J. Med. Chem.* 2013;69:762–767.
6. Badavath VN, Ipek B, Ucar G, Sinha BN, Jayaprakash V. Monoamine oxidase inhibitory activity of novel pyrazoline analogues: curcumin based design and synthesis, *ACS Med. Chem. Lett.* 2016;7:56–61.
7. Badavath VN, Ucar G, Sinha BN, Mondal SK, Jayaprakash V. Monoamine oxidase inhibitory activity of novel pyrazoline analogues: Curcumin based design and synthesis-II, *Chem. Sel.* 2016;1:1–7.
8. Badavath VN, Ipek B, Ucar G, Mondal SK, Sinha BN, Jayaprakash V. MAO inhibitory activity of ferulic acid amides: curcumin based design and synthesis, *Arch. Pharm.* 2015;348:1–11.
9. Badavath VN, Sinha BN, Jayaprakash V. Design, in-silico docking and predictive ADME properties of novel pyrazoline derivatives with selective human MAO inhibitory activity. *Int. J. Pharm. Pharm. Sci.* 2015;7:277–282.
10. Badavath VN, Jadav SS, Pastorino B, et al. Synthesis and antiviral activity of 2-phenyl-4H-chromen-4-one derivatives against Chikungunya virus, *Lett. Drug Des. Discov.* 2016;13:1–6.
11. Chimenti F, Maccioni E, Secci D, et al. Synthesis, stereochemical identification, and selective inhibitory activity against human monoamine oxidase-B of 2-methylcyclohexylidene-(4-arylthiazol-2-yl)hydrazones, *J. Med. Chem.* 2008;51:4874–4880.
12. Yanez M, Fraiz N, Cano E, Orallo F. Inhibitory effects of cis-and transresveratrol on noradrenaline and 5-hydroxytryptamine uptake and on monoamine oxidase activity, *Biochem. Biophys. Res. Commun.* 2006;344:688–695.
13. Narender T, Venkateswarlu K, Badavath VN, Sarkar S. A new chemical access for 30-acetyl-40-hydroxychalcones using BF₃-Et₂O via a regioselective Claisen–Schmidt condensation and its application in the synthesis of chalcone hybrids, *Tetrahedron Lett.* 2011;52:5794–5798.
14. Jadav SS, Kaptein S, Ajay kumar T, et al., Design, synthesis, optimization and antiviral activity of a class of hybrid dengue virus E protein inhibitors, *Bioorg. Med. Chem. Lett.* 2015;25:1747–1752.
15. Venkateswarlu S, Panchagnula GK, Gottumukkala AL, Subbaraju GV. Synthesis, structural revision, and biological activities of 40-chloroaurone a metabolite of marine brownalga *Spatoglossum variabile*, *Tetrahedron.* 2007;63:6909–6914.
16. Chimenti F, Carradori S, Secci D, et al., Synthesis and inhibitory activity against human monoamine oxidase of N1-thiocarbamoyl-3,5-di(hetero)aryl-4,5-dihydro-(1H)-pyrazole derivatives, *Eur. J. Med. Chem.* 2010;45:800–804.
17. Marion Bradford M, Rapid A. sensitive method for the quantitation of microgram quantities of protein utilizing the principle of protein-dye binding. *Anal. Biochem.* 1976; 72 (1–2):248–254.
18. Badavath VN, Ciftci-Yabanoglu S, Bhakat S, et al. Mono amine oxidase inhibitory activity of 2-aryl-4H-chromen-4-ones, *Bioorg. Chem.* 2015;58:72–80.

© 2021 Saxena et al.; This is an Open Access article distributed under the terms of the Creative Commons Attribution License (<http://creativecommons.org/licenses/by/4.0>), which permits unrestricted use, distribution, and reproduction in any medium, provided the original work is properly cited.

Peer-review history:

The peer review history for this paper can be accessed here:
<https://www.sdiarticle5.com/review-history/82773>